



PERGAMON

International Journal of Heat and Mass Transfer 43 (2000) 1715–1734

International Journal of
**HEAT and MASS
TRANSFER**

www.elsevier.com/locate/ijhmt

Convergence and accuracy of Adomian's decomposition method for the solution of Lorenz equations

Peter Vadasz^{a,*}, Shmuel Olek^b

^aDepartment of Mechanical Engineering, University of Durban-Westville, Private Bag X54001, Durban 4000, South Africa

^bPlanning, Development and Technology Division, Israel Electric Corporation Ltd., P.O. Box 10, Haifa 31000, Israel

Received 20 April 1999; received in revised form 12 August 1999

Abstract

The convergence and accuracy of Adomian's decomposition method of solution is analysed in the context of its application to the solution of Lorenz equations which govern at lower order the convection in a porous layer (or respectively in a pure fluid layer) heated from below. Adomian's decomposition method provides an analytical solution in terms of an infinite power series and is applicable to a much wider range of heat transfer problems. The practical need to evaluate the solution and obtain numerical values from the infinite power series, the consequent series truncation, and the practical procedure to accomplish this task, transform the analytical results into a computational solution evaluated up to a finite accuracy. The analysis indicates that the series converges within a sufficiently small time domain, a result that proves to be significant in the derivation of the practical procedure to compute the infinite power series. Comparison of the results obtained by using Adomian's decomposition method with corresponding results obtained by using a numerical Runge–Kutta–Verner method show that both solutions agree up to 12–13 significant digits at subcritical conditions, and up to 8–9 significant digits at certain supercritical conditions, the critical conditions being associated with the loss of linear stability of the steady convection solution. The difference between the two solutions is presented as projections of trajectories in the state space, producing similar shapes that preserve under scale reduction or magnification, and are presumed to be of a fractal form. © 2000 Elsevier Science Ltd. All rights reserved.

Keywords: Lorenz equations; Free convection; Weak turbulence; Chaos; Adomian's decomposition

1. Introduction

The application of Adomian's [1,2] decomposition method as an alternative solution method to a wide

variety of heat transfer problems motivates this study. The method is applicable to any heat transfer problem that can be reduced to a finite set of non-linear (or linear) ordinary differential equations, transforming an initial-boundary value problem which consists of partial differential equations, with their initial and boundary conditions, governing the heat transfer process, into an initial value (or boundary value) problem. While the applicability of the method to the problem of heat convection in a fluid layer heated from below was demonstrated by Vadasz [3], and its application to the corresponding problem in porous media by Vadasz

* Corresponding author. Tel.: +27-31-204-4873; fax: +27-31-204-4002.

E-mail address: vadasz@pixie.udw.ac.za (P. Vadasz).

¹ This work was undertaken while P. Vadasz was on Sabbatical leave as Visiting Professor at University of Natal-Durban, South Africa.

Nomenclature

Da	Darcy number, equals k_*/H_*^2	x	horizontal length co-ordinate
k_*	permeability of a porous matrix	y	horizontal width co-ordinate
H_*	the height of the domain	z	vertical co-ordinate
Pr	Prandtl number, ν_*/α_*	X	scaled amplitude
q	dimensionless velocity vector, equals $u\hat{e}_x + v\hat{e}_y + w\hat{e}_z$	Y	scaled amplitude
Ra	Rayleigh number	Z	scaled amplitude
R	scaled Rayleigh number, equals Ra/Ra_{cr}	<i>Greek symbols</i>	
Ra_{cr}	critical value of Rayleigh number associated with the loss of linear stability of the motionless solution	α_*	thermal diffusivity
R_t	value of R associated with the transition from steady to non-steady convection	β_*	thermal expansion coefficient
\hat{t}	time	ν_*	fluid's kinematic viscosity
T	dimensionless temperature, equals $(T_* - T_C)/(T_H - T_C)$	μ_*	fluid's dynamic viscosity
T_C	coldest wall temperature	ψ	stream function
T_H	hottest wall temperature	ϕ	porosity
u	horizontal x component of the velocity	t	rescaled time for porous media convection, equals $2\pi^2\hat{t}$
v	horizontal y component of the velocity	<i>Subscripts</i>	
w	vertical component of the velocity	$*$	dimensional values
		c	critical values
		t	transitional value

and Olek [4,5], particular questions regarding its convergence and accuracy remained unanswered. The objective of the present paper is to address these unanswered questions and compare the accuracy of the results obtained via Adomian's decomposition method with corresponding results obtained via classical numerical methods, such as the Runge–Kutta method. For demonstration purposes we adopted the solution of the Lorenz equations which govern at lower order the dynamics of convection in a fluid layer (or a fluid saturated porous layer) heated from below [6,7] and presents particular challenges due to its high sensitivity to small variations of the initial conditions on the threshold of transition from steady convection to weak-turbulence (chaos).

The derivation of Lorenz equations from the original partial differential equations was presented by Vadasz and Olek [4,5] for convection in a porous layer heated from below, and by Lichtenberg and Lieberman [8] and Vadasz [3] for the corresponding problem of convection in a pure fluid layer (non-porous domain) heated from below. There are different approaches to analyse the non-linear convection problem leading to different degrees of insight into the variety of phenomena and the corresponding dynamics of the system as the Rayleigh number increases. One such approach was adopted by Lorenz [6] (see also [7,8]). While the truncated Lorenz equations are limited either to moderate Rayleigh numbers or to represent the solution in the interior, excluding boundary layers which develop

at high values of Rayleigh number (Ra), Malkus [9] showed that in some cases this set of three equations decouple from the rest (with exact closure), at least in the sense of weighted residuals. Therefore, their solution is relevant even when solving at higher truncation levels as this set of three equations needs to be solved separately before attempting to solve the rest of the set corresponding to the higher modes. In general the dynamics related to this reduced system is so rich that it is important to understand it prior to attempting to solve at higher orders.

While most of the studies of Lorenz equations attempting to analyse the transition from steady convection to chaos use numerical methods, Vadasz and Olek [4,5] applied Adomian's decomposition method [1,2] to solve this set of equations for a porous layer heated from below at low and moderate Prandtl numbers, respectively. Similarly, the application of Adomian's decomposition method to solve the corresponding problem of centrifugally induced convection in a rotating porous layer was presented by Vadasz and Olek [10]. The decomposition method provides an analytical solution in terms of an infinite power series. The practical need to evaluate the solution and obtain numerical values from the infinite power series, the consequent series truncation, and the practical procedure to accomplish this task, transform the otherwise analytical results into a computational solution evaluated up to a finite accuracy. While Adomian's decomposition method was shown to provide extremely

accurate results for a wide range of non-linear problems (see [11]), it is necessary to investigate its accuracy particularly for problems which are known to possess properties of sensitivity of their solution to small variations in initial conditions. This provides the motivation for the present study.

2. Problem formulation and uniqueness of solution

The initial value problem considered in this paper consists of Lorenz equations presented in the form

$$\dot{X} = \alpha(Y - X) \tag{1a}$$

$$\dot{Y} = RX - Y - (R - 1)XZ \tag{1b}$$

$$\dot{Z} = 4\gamma(XY - Z) \tag{1c}$$

subject to the initial conditions;

$$t = 0: \quad X(0) = X_0; Y(0) = Y_0; Z(0) = Z_0 \tag{2}$$

where R is the scaled Rayleigh number defined as Ra/Ra_{cr} , where Ra_{cr} is the critical value of the Rayleigh number associated with the loss of stability of the motionless solution, and equals $Ra_{cr} = 4\pi^2$ for porous media convection, or $Ra_{cr} = 27\pi^4/4$ for convection in pure fluids. The parameter α is related to the Darcy–Prandtl number in porous media convection, i.e. $\alpha = \gamma\phi Pr/\pi^2 Da$, where $Da = k_*/H_*^2$ is the Darcy number, and it is equal to the Prandtl number Pr for convection in pure fluids. The parameter γ is related to the wave number of convection, which is taken to be consistent with the wave number at the convection threshold, a requirement imposed in order to fit the convection cells into the domain and fulfil the boundary conditions. This requirement yields for porous media convection a value of $\gamma = 1/2$, and for pure fluids convection (non-porous domains) $\gamma = 2/3$. With this value of γ the definitions of R and α are explicitly expressed in the form $R = Ra/4\pi^2$, $\alpha = \phi Pr/2\pi^2 Da$ for porous media convection, and $R = 4Ra/27\pi^4$, $\alpha = Pr$ for convection in pure fluids.

Lorenz Eqs. (1a)–(1c) represent at lower order the solution to the problem of convection in a fluid-saturated porous layer (or respectively in a pure fluid layer) of a dimensional height H_* and a thermal diffusivity (effective thermal diffusivity for porous media) α_* , heated from below. Its dependent variables X , Y and Z represent the amplitudes of the spatial modes for the dimensionless stream function and temperature expressed in the following form that applies to porous media convection

$$\psi = -\frac{2\sqrt{2\gamma(R-1)}}{\gamma} X(t) \sin(\pi x) \sin(\pi z) \tag{3}$$

$$T = 1 - z + \frac{2\sqrt{2\gamma(R-1)}}{\pi R} Y(t) \cos(\pi x) \sin(\pi z) - \frac{(R-1)}{\pi R} z(t) \sin(2\pi z) \tag{4}$$

where the rescaled time is presented in the form $t = 2\pi^2 \hat{t}$. Similar equations apply to convection in pure fluids (non-porous domains). This representation is equivalent to a Galerkin expansion of the solution in both x and z directions (dimensionless), truncated when $i+j=2$, where i is the Galerkin summation index in the x direction and j is the Galerkin summation index in the z direction.

Eqs. (1a)–(1c) are satisfied by the motionless solution $X = Y = Z = 0$ that is stable when $R < 1$, by the steady convective solutions $X = Y = \pm 1$ and $Z = 1$, which are linearly stable when $1 < R < R_{c2}$, and by chaotic or periodic solutions for values of, $R > R_t$, (with $R_t < R_{c2}$) where R_{c2} is the critical value of the scaled Rayleigh number associated with the loss of linear stability of the steady convection solution and can be presented in the form [3–5,7,12]

$$R_{c2} = \frac{\alpha(\alpha + 4\gamma + 3)}{(\alpha - 4\gamma - 1)} \tag{5}$$

and $R_t < R_{c2}$ is the actual transitional value of the scaled Rayleigh number when the transition from steady convection to chaos occurs. For $\alpha = 5$ and $\gamma = 1/2$ corresponding to porous media convection the loss of stability of the convection fixed points is evaluated using Eq. (5) to be $R_{c2} = 25$ and for initial conditions $X_0 = Y_0 = Z_0 = 0.9$ the transition occurs at $R = R_t = 24.647752$. The transition from the steady to the chaotic solution occurs via a subcritical Hopf bifurcation [3,7,12–14] and is associated with a homoclinic explosion when the trajectory which originally moves around one steady convective solution (fixed point) departs towards the other fixed point.

The system (1a)–(1c) has the general form $\dot{X} = f(X)$. By evaluating the Jacobian $(\partial f_i/\partial X_j)$ it is easy to observe that each term in the Jacobian matrix is bounded, i.e. it satisfies $(\partial f_i/\partial X_j) \leq M \forall \{t \in [0, t_{max}] \text{ and } [X \in \mathbb{R}^3]\}$, where $M > 0$ is Lipschitz constant. Therefore, for the system (1), $f(X)$ satisfies the Lipschitz continuity condition, hence the initial value problem (1a)–(1c) and (2) has a unique solution.

3. Adomian’s decomposition method of solution

Adomian’s decomposition method [1,2], is applied to

solve the initial value problem (1a)–(1c) and (2). The method provides in principle an analytical solution in the form of an infinite power series for each dependent variable and its excellent accuracy in solving non-linear equations was demonstrated by Olek [11]. The salient aspects of the method are presented in detail by Olek [11] or in a shorter form by Vadasz and Olek [4,5], and will therefore be skipped here. The method produces an analytical solution which takes the following form

$$X_i(t) = \sum_{n=0}^{\infty} c_{i,n} \frac{t^n}{n!} \quad \forall i = 1, 2, 3 \quad (6)$$

where $X_1 = X$, $X_2 = Y$ and $X_3 = Z$, and

$$c_{i,0} = X_i(0) \quad \forall i = 1, 2, 3 \quad (7)$$

and the general term for $n \geq 1$ is defined through the following recurrence relationship

$$c_{1,n} = -\alpha(c_{1,(n-1)} - c_{2,(n-1)}) \quad (8a)$$

$$c_{2,n} = Rc_{1,(n-1)} - c_{2,(n-1)} - (R - 1) \sum_{k=0}^{n-1} \frac{(n-1)! c_{1,k} c_{3,(n-k-1)}}{k!(n-k-1)!} \quad (8b)$$

$$c_{3,n} = -4\gamma c_{3,(n-1)} + 4\gamma \sum_{k=0}^{n-1} \frac{(n-1)! c_{1,k} c_{2,(n-k-1)}}{k!(n-k-1)!} \quad (8c)$$

While the form of the coefficients may cause incorrectly the misleading impression that the series solution (6) is just a Taylor expansion of the solution about $t = 0$, a careful inspection of Eqs. (8a)–(8c) shows that these coefficients are non-linearly coupled. Therefore this can not be a Taylor expansion of the solution in the usual sense except for particular cases when the relationships between the coefficients decouple. Actually, Adomian [2] showed that the sum of Adomian's polynomials that were used in the derivation of the analytical solution (6), is equal to a *generalised Taylor series about a function* $u_0(t)$ and this series converges very rapidly. One needs to distinguish here between the Taylor expansion of the solution about $t = 0$ which does not generally apply, and the generalised Taylor expansion about a function that Adomian [2] describes and applies generally to the derivation of the solution by using this method. These two are totally distinct concepts and they should be kept distinct to avoid confusion.

The practical need to evaluate numerical values from the infinite power series (6) suggests the use of the decomposition method as an algorithm for the approximation of the dynamical response in a sequence of time intervals $[0, t_1)$, $[t_1, t_2)$, \dots , $[t_{n-1}, t_n)$ such that the solution at t_p is taken as initial condition in the

interval $[t_p, t_{p+1})$ which follows. This approach has the following advantages: (i) in each time-interval one can apply a theorem proved by Répaci [15], which states that the solution obtained by the decomposition method converges to a unique solution as the number of terms in the series becomes infinite, and (ii) the approximation in each interval is continuous in time and can be obtained with the desired accuracy corresponding to the desired number of terms.

All computations in the following sections correspond to values of $\alpha = 5$, $\gamma = 1/2$ and initial conditions in the neighbourhood of the positive convective fixed point, i.e. $X_0 = Y_0 = Z_0 = 0.9$ (or $X_i(0) = 0.9 \forall i = 1, 2, 3$). These values correspond to a critical value of $R_{c2} = 25$ and a transitional value of $R_t = 24.647752$ (see [4]).

4. Convergence of the series solution

While Répaci [15], provides the rigorous proof of convergence of the series solution for a more general form of the problem, the objective in the present paper is to demonstrate the behaviour of this series (6) in more detail for the particular Lorenz equations (1). We are interested also in observing the changes in the series coefficients as the value of R varies from $R < 1$ corresponding to the motionless solution, via $1 \leq R < R_t$ corresponding to steady convection (the transition from steady convection to chaos occurs at a slightly subcritical value of $R = R_t < R_{c2}$) and up to supercritical values of $R > R_{c2}$.

The computation of the coefficients of the series solution (6) subject to the initial conditions $X_0 = Y_0 = Z_0 = 0.9$ (or $X_i(0) = 0.9 \forall i = 1, 2, 3$) was performed according to the recurrence Eqs. (8a)–(8c) by using *Mathematica*[®] [16]. The results show that the series consists of both positive and negative terms although not in a regular alternating fashion. While it seems that for large n values some multi-periodic variation of sign exists for some range of values of R we did not investigate in detail this behaviour. Instead, we applied the ratio test on the absolute values of the series coefficients. This provides a sufficient (although not necessary) condition for convergence of the series for a time interval $\Delta t = t_p - t_{p-1}$, in the form

$$\lim_{n \rightarrow \infty} \left| \frac{c_{i,n+1}}{(n+1)c_{i,n}} \right| < \frac{1}{\Delta t} \quad (9)$$

Therefore, if for each value of $R > 0$ there is a positive constant M which depends on R such that

$$\lim_{n \rightarrow \infty} \left| \frac{c_{i,n+1}}{(n+1)c_{i,n}} \right| < M \quad (10)$$

then there is always a value of $\Delta t > 0$ for which the original series (6) converges unconditionally, i.e. $\Delta t = 1/M$. Instead of attempting to prove inequality (10) we prefer to demonstrate the convergence of the series by replacing $\lim_{n \rightarrow \infty} |c_{i,n+1}/(n+1)c_{i,n}|$ with $\lim_{n \rightarrow N} |c_{i,n+1}/(n+1)c_{i,n}|$ in Eq. (9) where $N \rightarrow$ large constant, and observe the behaviour of the function $f(n) = |c_{i,n+1}/(n+1)c_{i,n}|$ as the value of n increases. The results of the evaluated values of $f(n)$ for $n = 1, 2, 3, \dots, N$ (where $N = 500$) corresponding to different values of R , are presented in Fig. 1. The results corresponding to the motionless solution were evaluated for $R = 0.9$ and are presented in Fig. 1(a). It is clear from this figure that the ratio $f(n)$ decays as n increases indicating obviously that condition (9) is satisfied and the series converges. Increasing the value of R to slightly supercritical conditions corresponding to $R = 1.1$ provides the results presented in Fig. 1(b), where the detail presented as the inset in Fig. 1(c) shows a quite regular pattern of this ratio at high values of n . Clearly there is no evidence of any divergence trend for the ratio $f(n)$, while its maximum value in this domain is smaller than 50. Similar results apply for $R = 5$ which corresponds to an oscillatory decaying solution towards the convective steady state (see [4]) as presented in Fig. 1(d). Its detail presented as the inset in Fig. 1(e) shows also a quite regular pattern at high values of n . As the value of R gets closer to the transition from steady convection to chaos it can be observed that the regularity of the ratio $f(n)$ disappears as presented in Fig. 1(f) for $R = 23 < R_t$. Nevertheless, this ratio remains bounded and there is no indication of divergence as the value of n increases. Similarly, the ratio $f(n)$ remains bounded even for conditions pertaining to chaotic solutions as presented in Fig. 1(g) corresponding to $R = 25 > R_t$. We performed these evaluation up to values of $N = 1500$ (not shown here) with similar conclusions. While this does not provide a rigorous proof as we did not evaluate the limit for $n \rightarrow \infty$ but rather for $n \rightarrow N$ where N is a very large number, there is no evidence of a trend of divergence of $f(n)$. However, in order to provide a more substantial evidence that Adomian's decomposition method not only converges but is also accurate when a much smaller number of terms is used we are providing in the next section a comparison between the Adomian's decomposition results (referred thereafter as "the computational results") and a numerical solution obtained by using the Runge–Kutta–Verner method (referred thereafter as "the numerical results").

5. Accuracy of Adomian's decomposition solution

In order to investigate the accuracy of Adomian's

decomposition method of solution we adopted a two-fold strategy. First, we show that the Adomian decomposition solution to a reduced version of Eqs. (1a)–(1c), which has a closed form solution as well, yields results identical to the closed form solution. Second, we solve the system (1a)–(1c) and (2) numerically and compare the numerical results to Adomian decomposition results. The adopted numerical method of solution is the fifth and sixth order Runge–Kutta–Verner scheme from the IMSL Library (DIVPRK) [17] which was applied to double precision to solve the system (1a)–(1c) and (2) up to a desired tolerance for error control specified by the parameter *tol*.

5.1. Solution to a one-dimensional version of the equations

In the particular case of a reduced one-dimensional non-linear system similar to (1a)–(1c), the problem reduces to

$$\frac{dX}{dt} = bX + aX^2 \tag{11}$$

which has the closed-form solution (obtained by a simple integration)

$$X = \frac{bX_0 e^{bt}}{[b + aX_0(1 - e^{bt})]} \tag{12}$$

where X_0 is the initial condition representing the value of X at $t = 0$. The Taylor expansion of this closed-form solution (12) takes the form

$$\begin{aligned} X(t) &= X_0 + X'(0)t + \frac{X''(0)t^2}{2} + \dots + \frac{X^{(n)}(0)t^n}{n!} + \dots \\ &= X_0 + X_0(b + aX_0)t + X_0(b + aX_0)(b + 2aX_0)\frac{t^2}{2} \\ &\quad + X_0(b^3 + 7ab^2X_0 + 12a^2bX_0^2 + 6a^3X_0^3)\frac{t^3}{6} \dots \end{aligned} \tag{13}$$

On the other hand Adomian's decomposition solution applied to this case (i.e. to Eq. (11)) yields the coefficients $c_0 = X_0$ and

$$\begin{aligned} c_n &= bc_{n-1} + a \sum_{k=0}^{n-1} \frac{(n-1)!c_k c_{(n-k-1)}}{k!(n-k-1)!} \quad \forall \\ n &= 1, 2, 3, \dots \end{aligned} \tag{14}$$

for the solution

$$X = \sum_{n=0}^{\infty} c_n \frac{t^n}{n!} \tag{15}$$

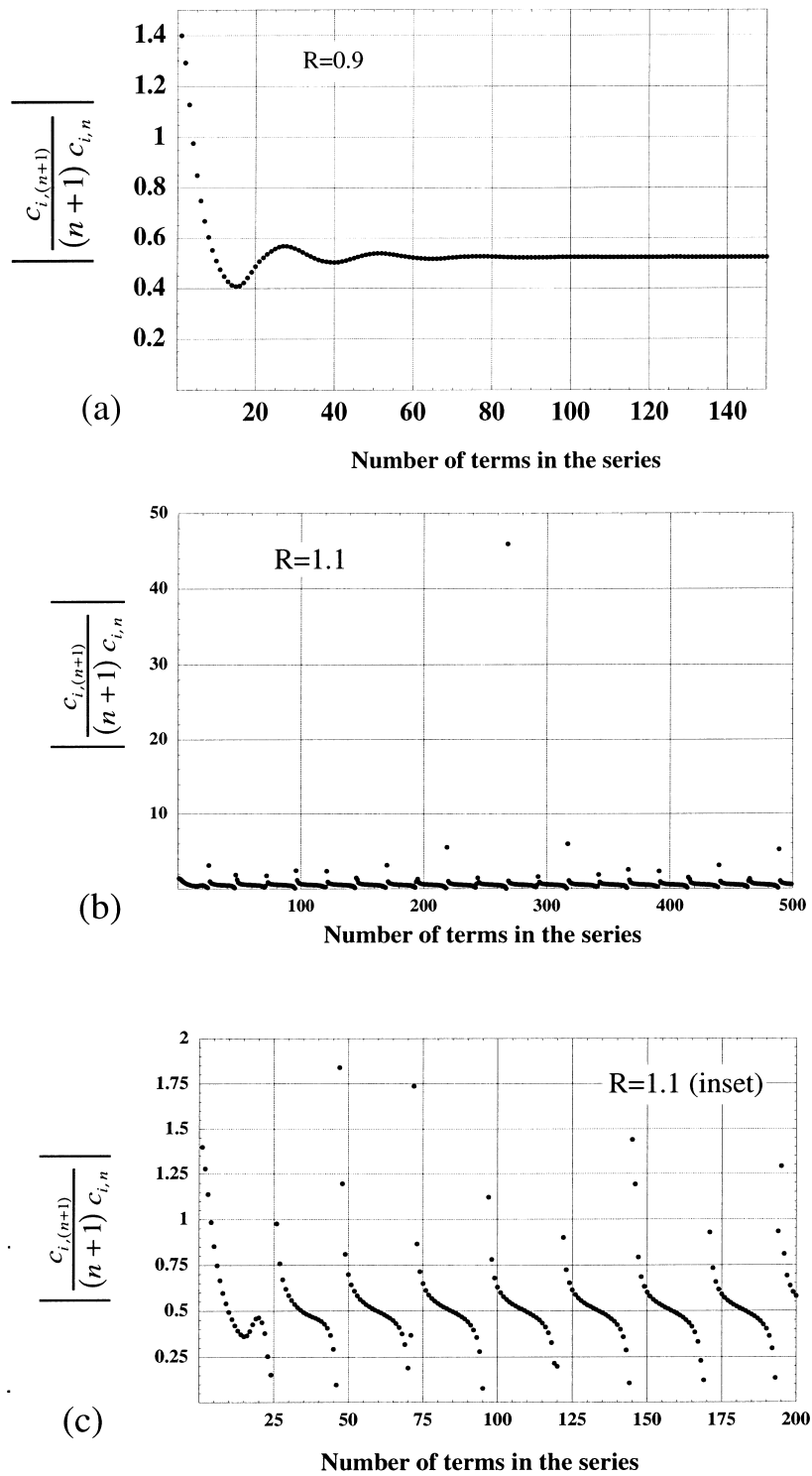


Fig. 1. The ratio convergence test applied to the series coefficients for Adomian's decomposition solution, as a function of the number of terms in the series, corresponding to (a) $R = 0.9$, (b) $R = 1.1$, (c) inset for $R = 1.1$, (d) $R = 5$, (e) inset for $R = 5$, (f) $R = 23$, (g) $R = 25$.

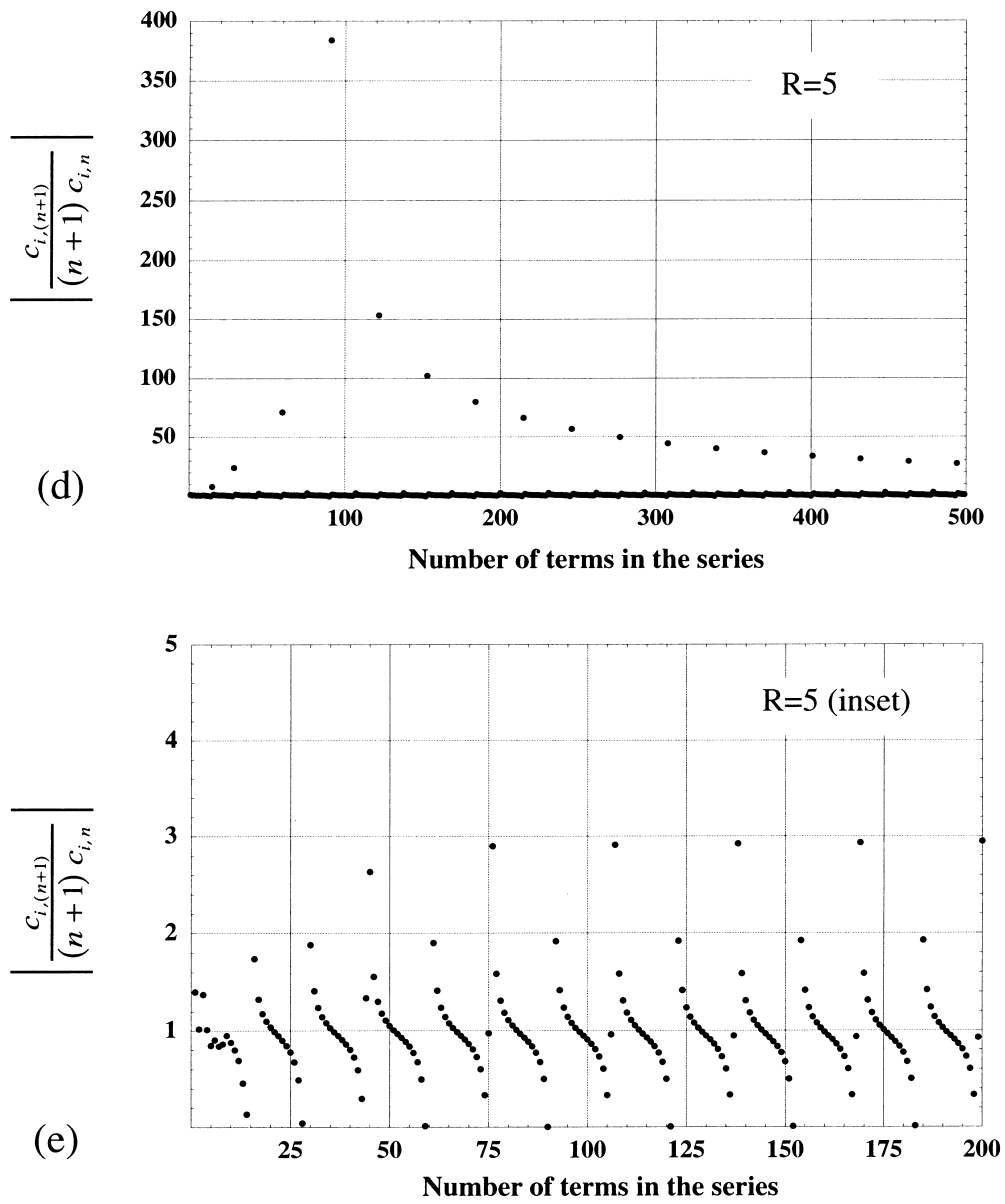


Fig. 1 (continued)

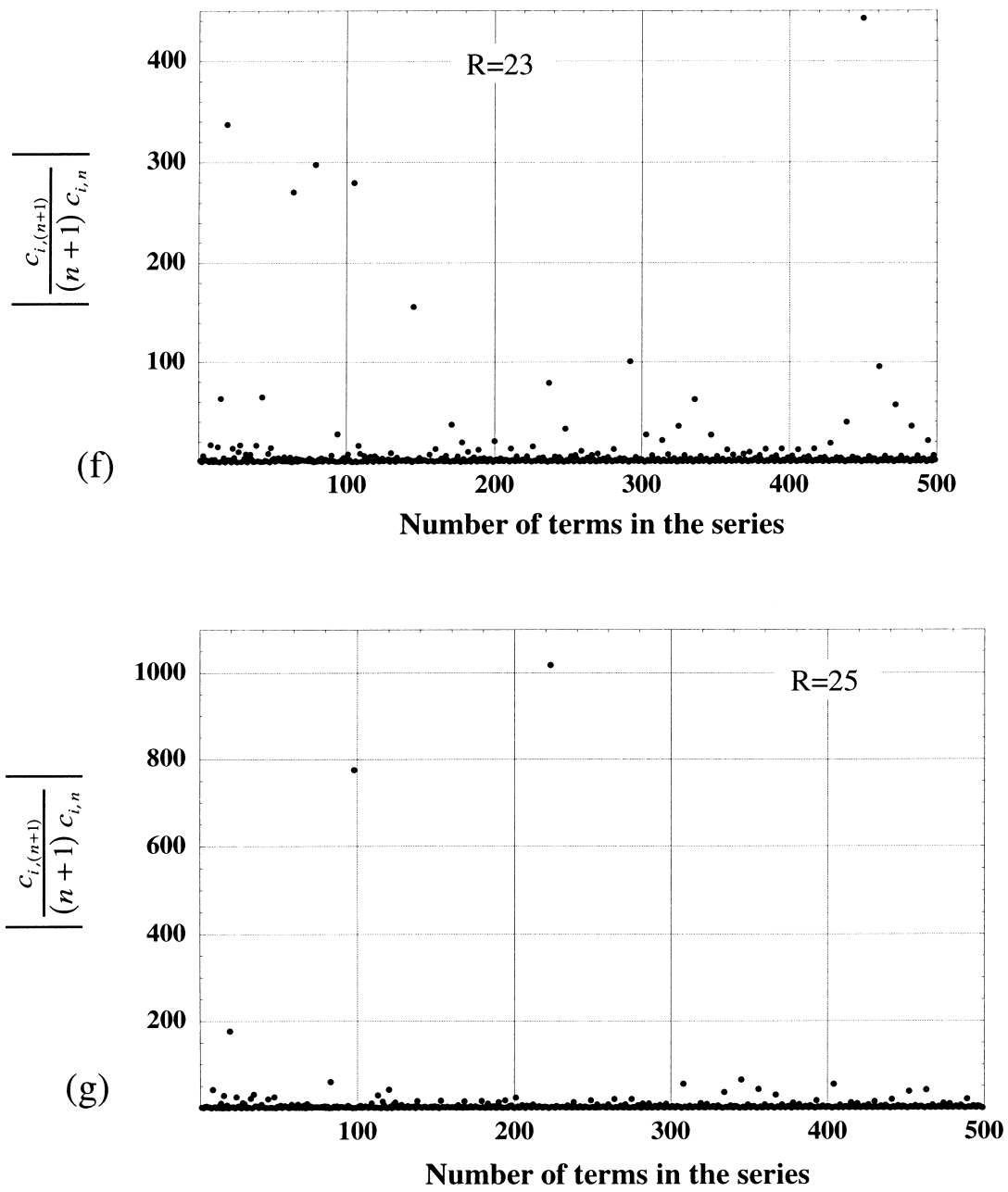


Fig. 1 (continued)

By evaluating explicitly the coefficients in Eq. (14) and substituting them into Eq. (15) yields the following solution

$$X(t) = X_0 + X_0(b + aX_0)t + X_0(b + aX_0)(b + 2aX_0)\frac{t^2}{2} + X_0(b^3 + 7ab^2X_0 + 12a^2bX_0^2 + 6a^3X_0^3)\frac{t^3}{6} \dots \quad (16)$$

This is indeed identical to the Taylor expansion (13) about $t = 0$, of the closed form solution (12) to Eq. (11). Therefore, for this reduced one-dimensional non-linear system (11), Adomian's decomposition method yields a Taylor expansion of the closed-form solution (12), recovering the accurate solution. For equivalent systems of higher dimensions, however, one can not generally expect Adomian's decomposition solution to reduce to a simple Taylor expansion in the usual sense.

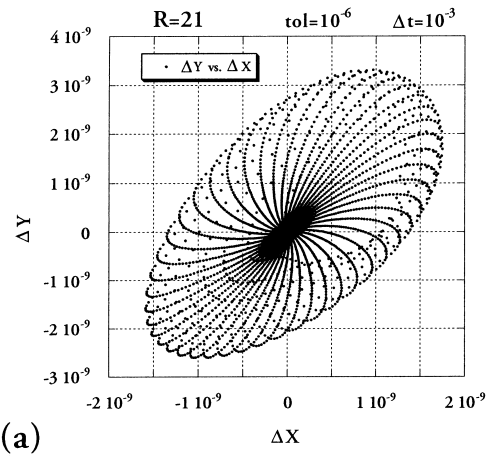
5.2. Solution to the complete three-dimensional system

In contrast to the one-dimensional system, for the complete three-dimensional system of Eqs. (1a)–(1c) and (2) representing the original initial value problem corresponding to Lorenz equations we can not expect a closed form solution and consequently Adomian's decomposition solution to provide a Taylor expansion of the solution in the usual sense. For this case we solved the system (1a)–(1c) and (2) numerically to double precision by using the fifth and sixth order Runge–Kutta–Verner method from the IMSL Library (DIVPRK) [17] up to a desired tolerance for error control specified by the parameter *tol*. We then compared the Adomian decomposition results (referred thereafter as “the computational results”) with the numerical solution (referred thereafter as “the numerical results”) by evaluating the difference between the two at all values of t up to $t_{\max} = 210$ and plotting this difference in the results as projections of the trajectory of differences on the planes $\Delta Z = 0$ ($\Delta Y - \Delta X$ plane), $\Delta Y = 0$ ($\Delta Z - \Delta X$ plane) and $\Delta X = 0$ ($\Delta Z - \Delta Y$ plane), where $\Delta X = X_{\text{comp.}} - X_{\text{num.}}$, $\Delta Y = Y_{\text{comp.}} - Y_{\text{num.}}$ and $\Delta Z = Z_{\text{comp.}} - Z_{\text{num.}}$. The indices “comp.” and “num.” stand for representing the computational (Adomian decomposition) and numerical (Runge–Kutta) results, respectively. However, just before undertaking this comparison we assessed the impact of the number of terms in the series solution, and its truncation, on the results by evaluating the Adomian decomposition results for $R = 21$ and $R = 75$ with 15 and 150 terms in the series and comparing them. The results of this comparison expressed as $X_{(15)}$ versus $X_{(150)}$, showed that their numerical values are identical over the whole range of significant digits of the double precision computation. We therefore concluded that it is sufficiently

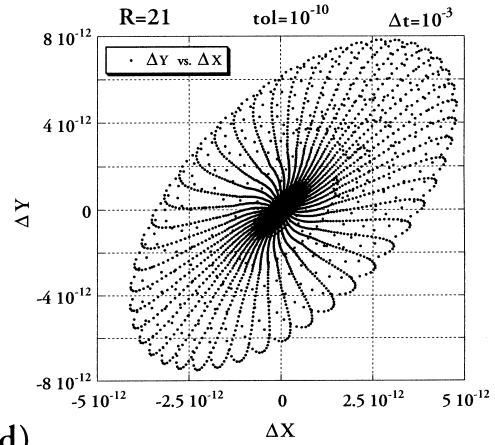
accurate for the following computations to use 15 terms in the series for the computational solution.

The results of the comparison between the computational and numerical solutions corresponding to a value of $\Delta t = 10^{-3}$ used in the computational solution, and to a value of the tolerance control parameter *tol* = 10^{-6} used in the numerical solution, and for $R = 21$, are presented in Fig. 2(a), (b) and (c). From these figures it is evident that the difference between the computational and numerical solutions is of the order of magnitude 10^{-9} . Attempting to increase the accuracy of the numerical solution by decreasing the value of the tolerance control parameter to *tol* = 10^{-10} and keeping the value of Δt unchanged, i.e. $\Delta t = 10^{-3}$, yields the results presented in Fig. 2(d), (e) and (f) in terms of projections of trajectories data points on the planes $\Delta Z = 0$, $\Delta Y = 0$ and $\Delta X = 0$, where the data points are not connected. It can be observed from these figures that increasing the accuracy of the numerical solution brought the computational and numerical results closer to each other up to an order of magnitude of 10^{-12} (for the maximum difference between the two). In addition one can observe by comparing the Fig. 2(a) with (d), (b) with (e) and (c) with (f) that the shape of the trajectory of differences is kept quite similar under the scale reduction which resulted from increasing the accuracy of the numerical solution. A further attempt to increase the accuracy of the numerical solution by reducing the tolerance control parameter to *tol* = 10^{-12} (which is the smallest possible value that produces valid results) and evaluating the differences between the numerical and computational solutions yields the results as presented in Fig. 3. It is evident that the maximum difference is now of an order of magnitude of 10^{-13} , as can be observed from Fig. 3(a), (b) and (c). Their corresponding results in the time domain are presented in Fig. 3(d) representing the envelope of the solution $\Delta X(t)$, and their details are highlighted as insets for different time ranges in Fig. 3(e) and (f).

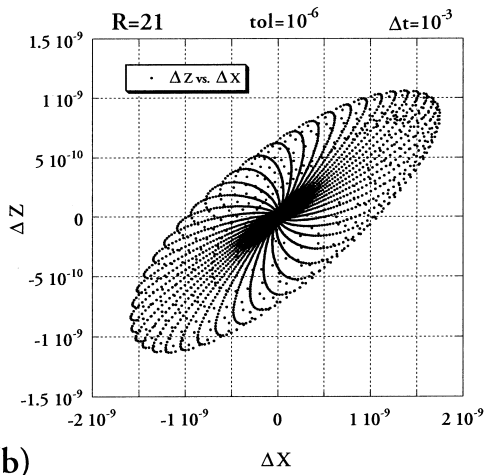
Up to this point the comparison between the computational and numerical results shows that by increasing the accuracy of the numerical solution (i.e. decreasing the value of the tolerance control parameter) brings its results closer to the computational solution up to a maximum difference between the two of an order of magnitude of 10^{-13} . These results correspond to steady convection, i.e. subcritical conditions ($R = 21$). Naturally, one can not expect similar results for supercritical conditions when the solution is chaotic, because then two nearby trajectories diverge (at least one of their Lyapunov exponents is positive). In order to compare the results between the numerical and computational solutions and establish the accuracy of Adomian's decomposition method at supercritical conditions we use the existence of periodic windows



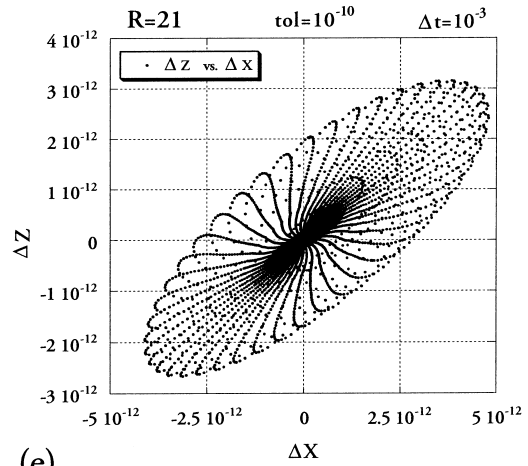
(a)



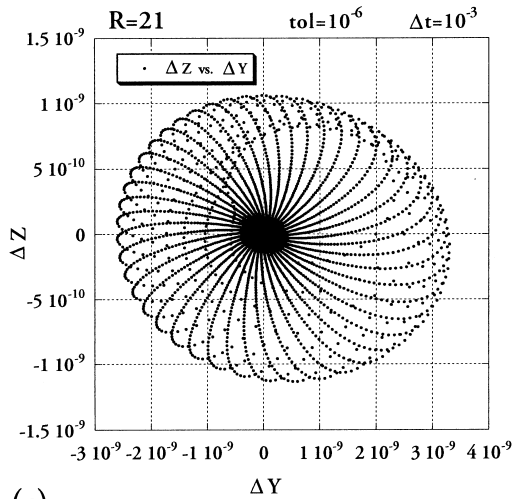
(d)



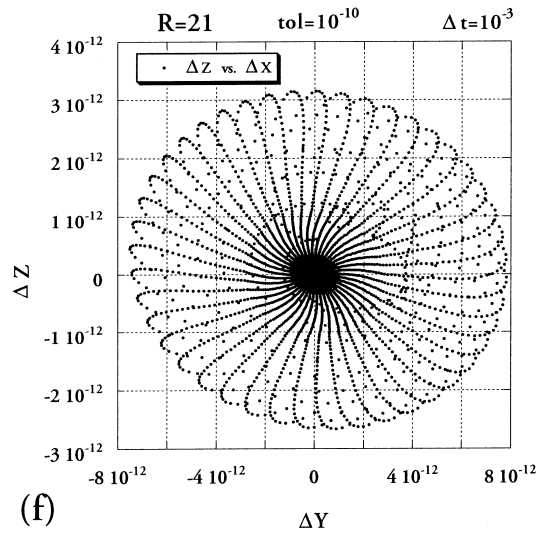
(b)



(e)



(c)



(f)

Fig. 2. Trajectory of differences between the computational (Adomian decomposition) and numerical (Runge–Kutta) solutions corresponding to $\Delta t = 10^{-3}$ in the computational solution, and $R = 21$. (a) Projection of trajectory's data points on the plane $\Delta Z = 0$, with $\text{tol} = 10^{-6}$ in the numerical solution, (b) projection of trajectory's data points on the plane $\Delta Y = 0$, with $\text{tol} = 10^{-6}$ in the numerical solution, (c) projection of trajectory's data points on the plane $\Delta X = 0$, with $\text{tol} = 10^{-6}$ in the numerical solution, (d) projection of trajectory's data points on the plane $\Delta Z = 0$, with $\text{tol} = 10^{-10}$ in the numerical solution, (e) projection of trajectory's data points on the plane $\Delta Y = 0$, with $\text{tol} = 10^{-10}$ in the numerical solution, (f) projection of trajectory's data points on the plane $\Delta X = 0$, with $\text{tol} = 10^{-10}$ in the numerical solution. (Data points are not connected.)

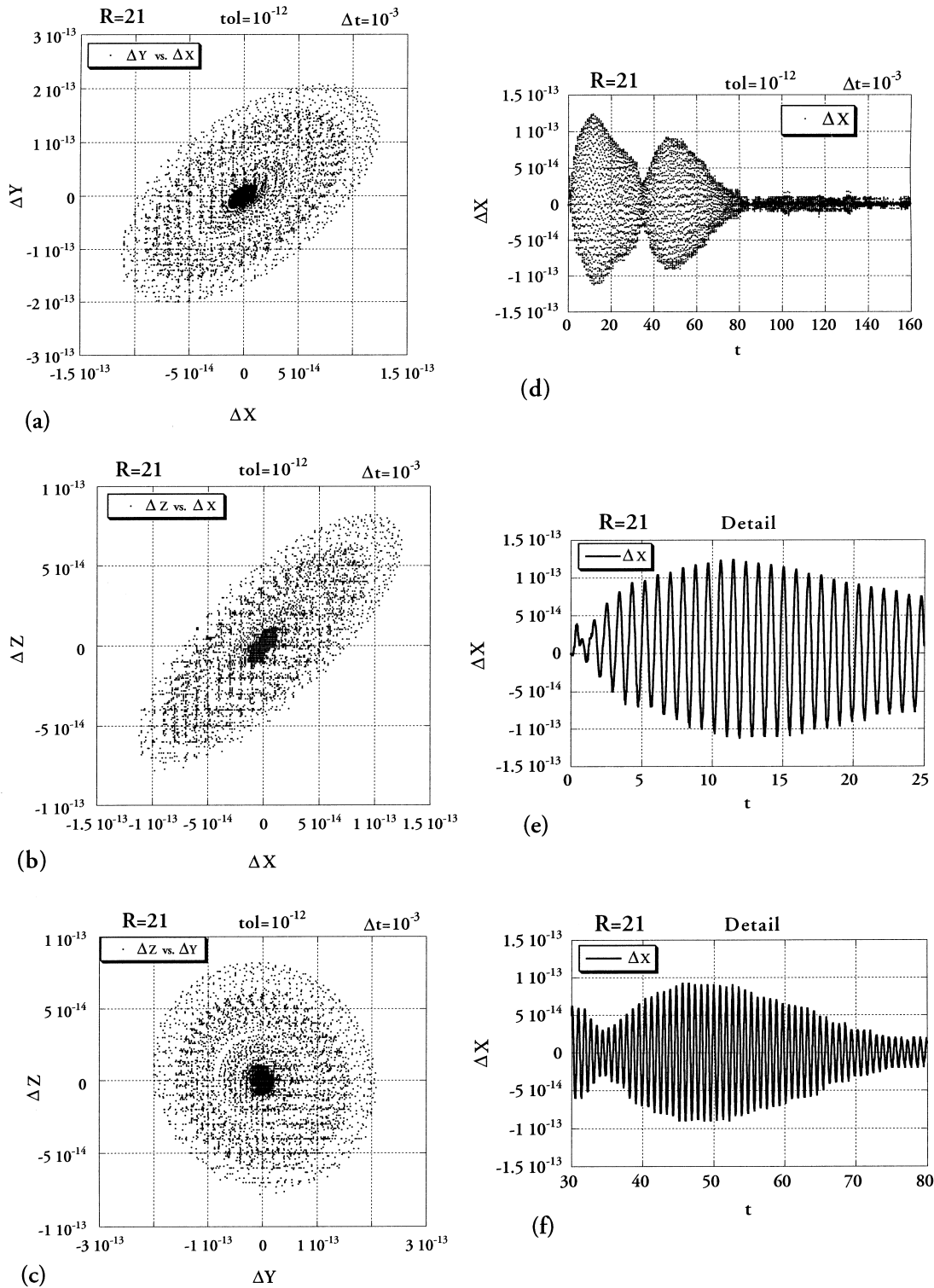


Fig. 3. Trajectory of differences between the computational (Adomian decomposition) and numerical (Runge–Kutta) solutions corresponding to $\Delta t = 10^{-3}$ in the computational solution, $\text{tol} = 10^{-12}$ in the numerical solution, and $R = 21$. (a) Projection of trajectory's data points on the plane $\Delta Z = 0$, (b) projection of trajectory's data points on the plane $\Delta Y = 0$, (c) projection of trajectory's data points on the plane $\Delta X = 0$, (d) the solution of $\Delta X(t)$ projected on the time domain, (e) inset of the solution $\Delta X(t)$ projected on the time domain for $0 < t < 25$, (f) inset of the solution $\Delta X(t)$ projected on the time domain for $30 < t < 80$. (Except for (e) and (f), the data points are not connected.)

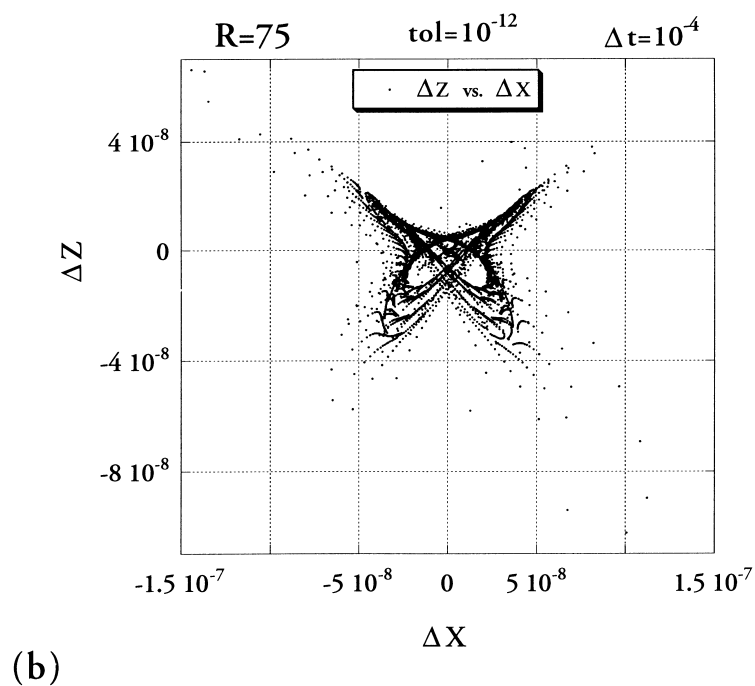
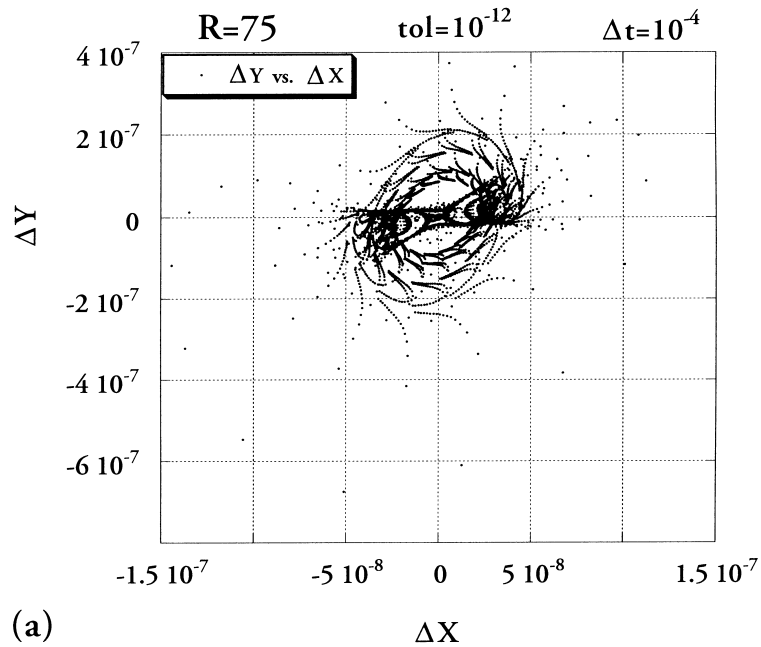


Fig. 4. Trajectory of differences between the computational (Adomian decomposition) and numerical (Runge–Kutta) solutions corresponding to $\Delta t = 10^{-4}$ in the computational solution, $\text{tol} = 10^{-12}$ in the numerical solution, and $R = 75$. (a) Projection of trajectory's data points on the plane $\Delta Z = 0$, (b) projection of trajectory's data points on the plane $\Delta Y = 0$, (c) projection of trajectory's data points on the plane $\Delta X = 0$, (d) inset of the projection of trajectory's data points on the plane $\Delta X = 0$. (Data points are not connected.)

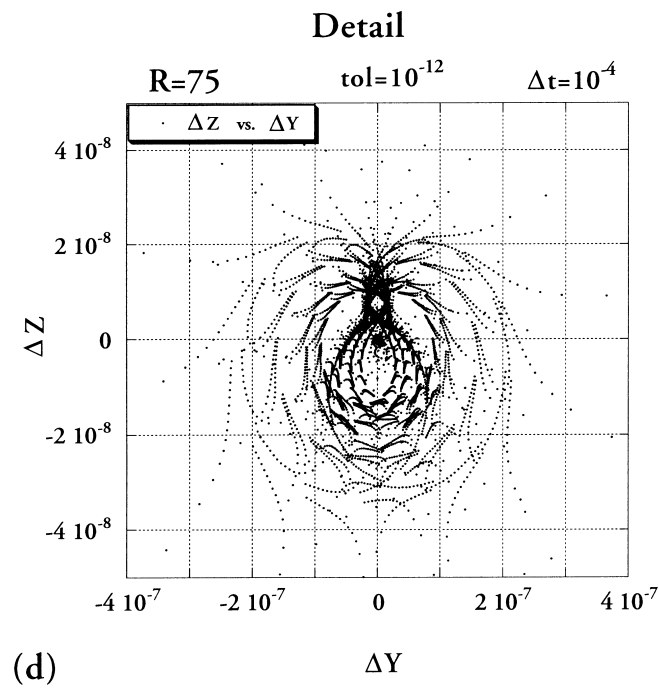
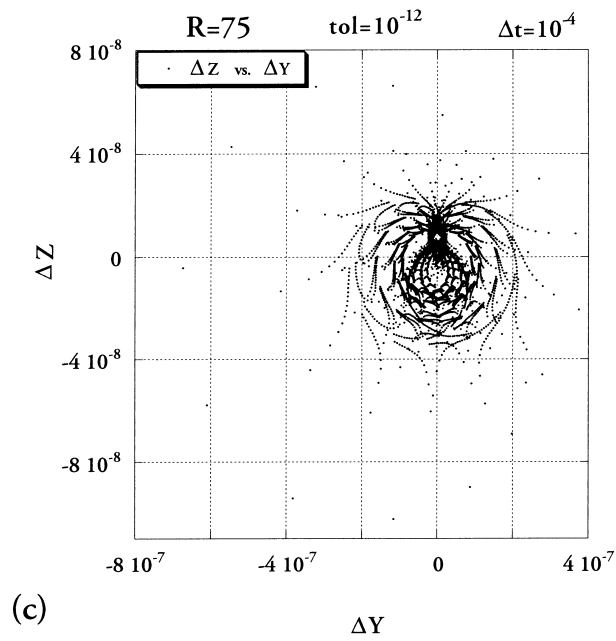


Fig. 4 (continued)

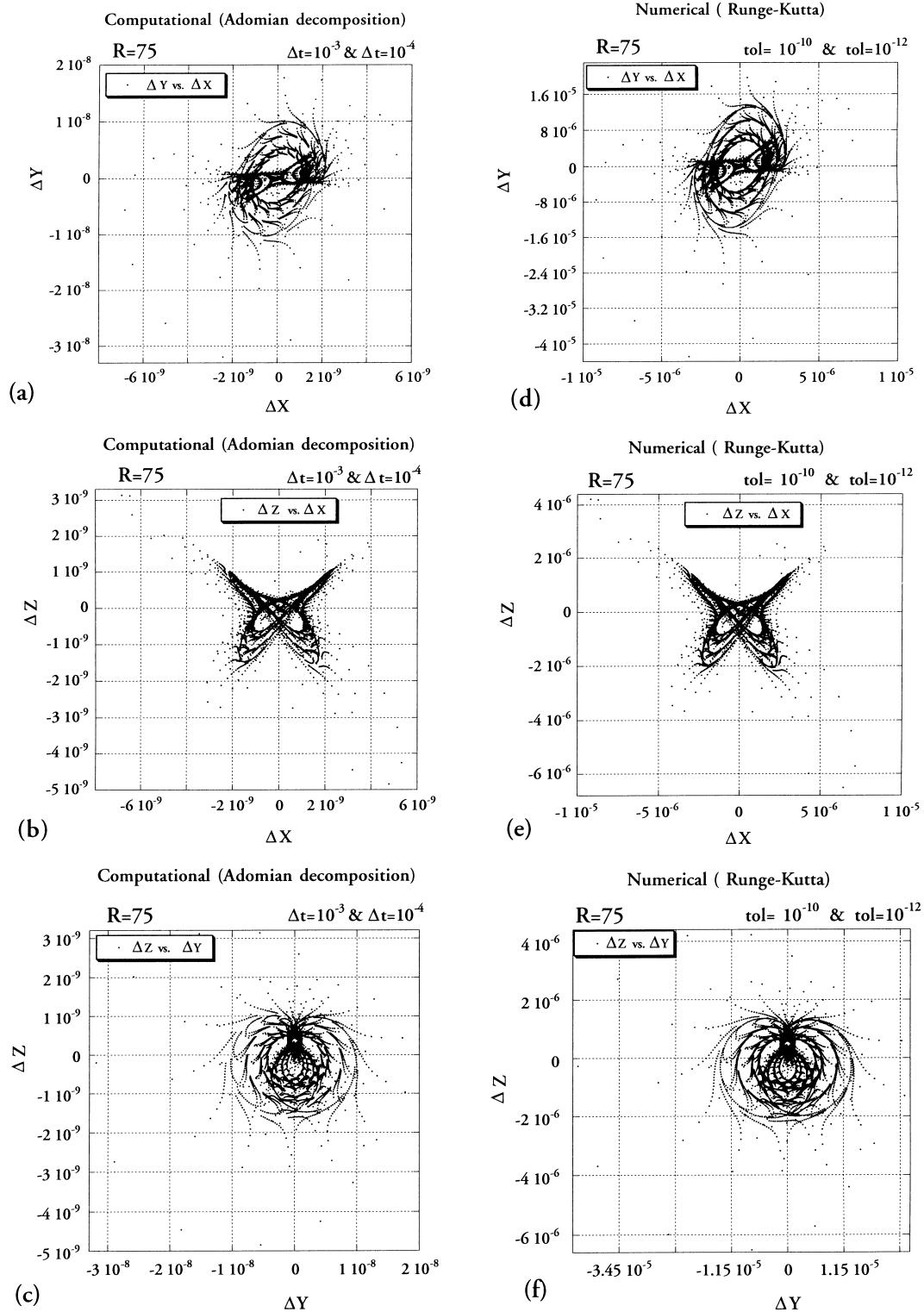


Fig. 5. Trajectory of differences between the computational (Adomian decomposition) results corresponding to $\Delta t = 10^{-3}$ and $\Delta t = 10^{-4}$ for $R = 75$. (a) Projection of trajectory's data points on the plane $\Delta Z = 0$, (b) projection of trajectory's data points on the plane $\Delta Y = 0$, (c) projection of trajectory's data points on the plane $\Delta X = 0$. Trajectory of differences between the numerical (Runge-Kutta) results corresponding to $\text{tol} = 10^{-10}$ and $\text{tol} = 10^{-12}$ for $R = 75$ (d) projection of trajectory's data points on the plane $\Delta Z = 0$, (e) projection of trajectory's data points on the plane $\Delta Y = 0$, (f) projection of trajectory's data points on the plane $\Delta X = 0$. (Data points are not connected.)

within the chaotic regime and evaluate the comparison at values of R corresponding to these periodic windows. The first wide periodic window appears around $R = 75$ (see [4]).

We evaluate therefore the differences between the computational and numerical solutions ΔX , ΔY and ΔZ at $R = 75$ providing the results presented in Fig. 4(a), (b) and (c) in terms of projections of trajectories data points on the planes $\Delta Z = 0$, $\Delta Y = 0$ and $\Delta X = 0$, where the data points are not connected. A value of $\Delta t = 10^{-4}$ was used in the computational solution, and a value of the tolerance control parameter $\text{tol} = 10^{-12}$ was used in the numerical solution for the results presented in Fig. 4. It can be observed from the figures that the maximum difference between the two solutions is of the order of magnitude of 10^{-7} . In addition the detail of the trajectory of differences projected on the plane $\Delta X = 0$ is presented as the inset of Fig. 4(c) in Fig. 4(d) where a better description of the shape of the trajectory can be observed. At this stage we were interested to establish the reason for the greater difference between the solutions as compared with the results obtained at subcritical conditions, i.e. for $R = 21$, and in particular we attempted to establish which one of the solutions, the computational or the numerical is to be “blamed” for increasing the difference between the two from $O(10^{-13})$ at $R = 21$ to $O(10^{-7})$ at $R = 75$. In order to establish this we evaluated the differences between two consecutive computational solutions corresponding to $\Delta t = 10^{-3}$ and $\Delta t = 10^{-4}$, respectively, and two consecutive numerical solutions corresponding to $\text{tol} = 10^{-10}$ and $\text{tol} = 10^{-12}$ respectively. The differences between the two computational solutions are presented in Fig. 5(a), (b) and (c) and the differences between the numerical solutions are presented in Fig. 5(d), (e) and (f). It is evident from Fig. 5 that the maximum difference in the computational solution is of the order of magnitude $O(10^{-9})$ while the maximum difference in the numerical solution is of the order of magnitude $O(10^{-5})$. We can therefore establish that the computational solution is more accurate in this case (i.e. its level of accuracy is saturated) and the “blame” for the loss of accuracy is to be placed on the numerical solution. Naturally, one can improve the accuracy of the numerical method by adopting a constant rather than variable time step algorithm, which is less efficient computationally, or by choosing a higher order Runge–Kutta scheme. Nevertheless, the comparison offered here is related to a standard library package (IMSL DIVPRK [17]) that is likely to be widely used. In this context, the comparison shows that when the standard library package tolerance parameter is taken to its limit (no more tightening of tolerance is possible beyond $\text{tol} = 10^{-12}$), the computational solution outperforms the numerical one. Furthermore, even when we decrease the

number of terms in the series to 10 the computational results remain the same up to the whole range of digits of machine precision. Therefore, the computational results are more accurate than the presently used numerical ones corresponding to their smallest possible tolerance, even with only 10 terms in the series. Reducing further the number of terms in the series decreases the accuracy of the computational results. An additional interesting result which is evident from Fig. 5 is that the shape of the trajectory of differences is kept similar under the scale reduction.

We continued to compare the computational and numerical solutions at the next wide periodic window (see [4]), i.e. at $R = 86$ with the parameters $\Delta t = 10^{-4}$ for the computational solution and $\text{tol} = 10^{-12}$ for the numerical solution. Their results are presented in Fig. 6 where a further deviation between the two solutions is evident resulting in a maximum difference of an order of magnitude of $O(10^{-3})$. Finally, we computed the difference between the two solutions (computational and numerical) for the post-chaotic regime obtained at high R values (see [4,7]). The results for the differences in this regime for $R = 150$ (with $\Delta t = 10^{-4}$ for the computational solution and $\text{tol} = 10^{-12}$ for the numerical solution) are presented in Fig. 7(a), (b) and (c) showing a maximum difference of an order of magnitude of $O(10^{-10})$. Their corresponding solutions in the time domain are presented for ΔX versus t in Fig. 7(d) and for ΔY versus t in Fig. 7(e). The detail of Fig. 7(e) representing the inset of the solution in the time interval $200 < t < 210$ is presented in Fig. 7(f). The results in the time domain clearly indicate that the differences between the solutions continue to increase, while in a small time interval ($200 < t < 210$) this difference seems almost periodic. The linear shape of the solution envelope function in the time domain is particularly interesting to notice. In order to establish the further evolution of the differences solution in time we re-evaluated both the computational and the numerical solutions up to a maximum time of $t_{\text{max}} = 650$, i.e. more than three times longer than the previous. The results of the differences for this long time solutions are presented in Fig. 8 showing a maximum difference of an order of magnitude of $O(10^{-9})$. Therefore increasing the maximum time for the computations by a factor of ~ 3 increased the difference between the two solutions by one order of magnitude. Another result observed from comparing Fig. 8(a), (b) and (c) with Fig. 7(a), (b) and (c) is that the shape of the trajectory of differences is altered only in the sense that a flip around the plane $\Delta Z = 0$ occurred, but the shape presented in Fig. 7 is included at the lower scale in Fig. 8, hence the shape is preserved similar under reduction or magnification and is therefore presumed to be a fractal. The corresponding results for the long time solutions are presented in Fig. 8(d), (e) and (f),

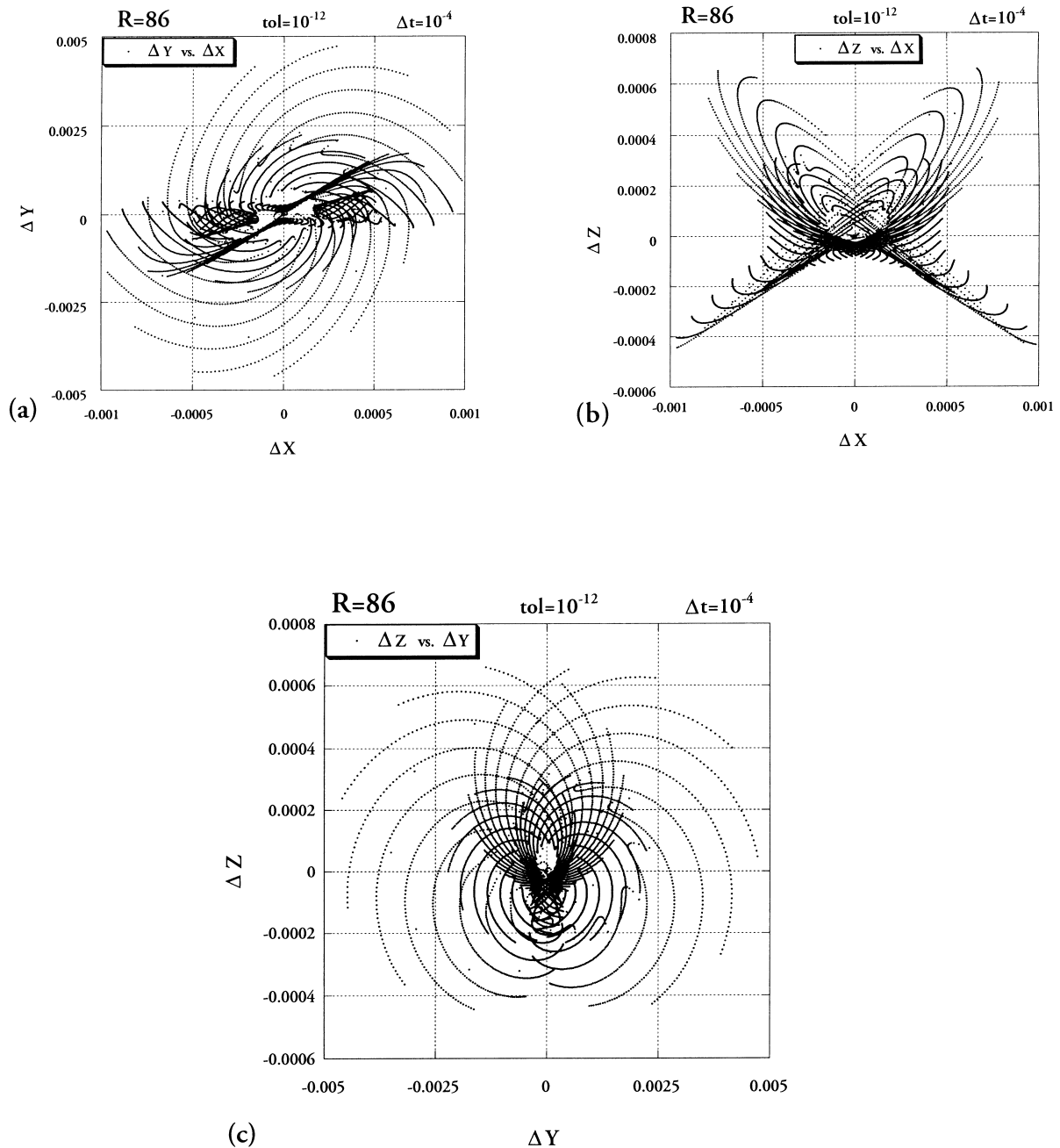


Fig. 6. Trajectory of differences between the computational (Adomian decomposition) and numerical (Runge–Kutta) solutions corresponding to $\Delta t = 10^{-4}$ in the computational solution, $\text{tol} = 10^{-12}$ in the numerical solution, and $R = 86$. (a) projection of trajectory's data points on the plane $\Delta Z = 0$, (b) projection of trajectory's data points on the plane $\Delta Y = 0$, (c) projection of trajectory's data points on the plane $\Delta X = 0$. (Data points are not connected.)

where the inset corresponding to the detailed time interval $646 < t < 650$ is presented in Fig. 8(e), identifying what seems to be an almost periodic behaviour. It is evident from the time domain representations of

the solutions that increasing the maximum time for the computation does not bring the solution differences to a post-transient state.

These differences continue to increase as t increases

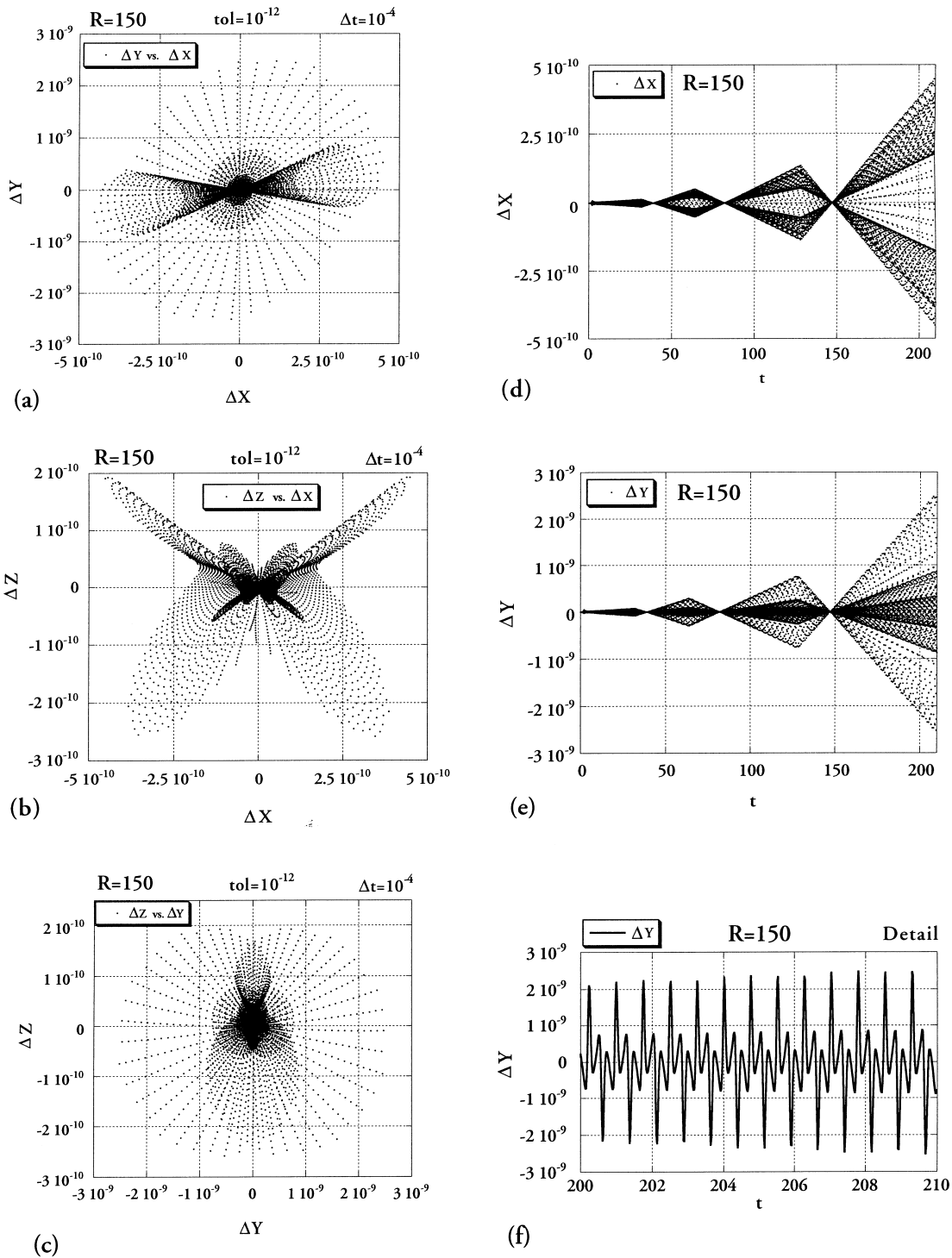


Fig. 7. Trajectory of differences between the computational (Adomian decomposition) and numerical (Runge–Kutta) solutions for a maximum computational time, $t_{\max}=210$, corresponding to $\Delta t=10^{-4}$ in the computational solution, $\text{tol}=10^{-12}$ in the numerical solution, and $R=150$. (a) Projection of trajectory's data points on the plane $\Delta Z=0$, (b) projection of trajectory's data points on the plane $\Delta Y=0$, (c) projection of trajectory's data points on the plane $\Delta X=0$. (d) the solution of $\Delta X(t)$ projected on the time domain, (e) the solution of $\Delta Y(t)$ projected on the time domain, (f) inset of the solution $\Delta Y(t)$ projected on the time domain for $200 < t < 210$. (Except for (f), the data points are not connected.)

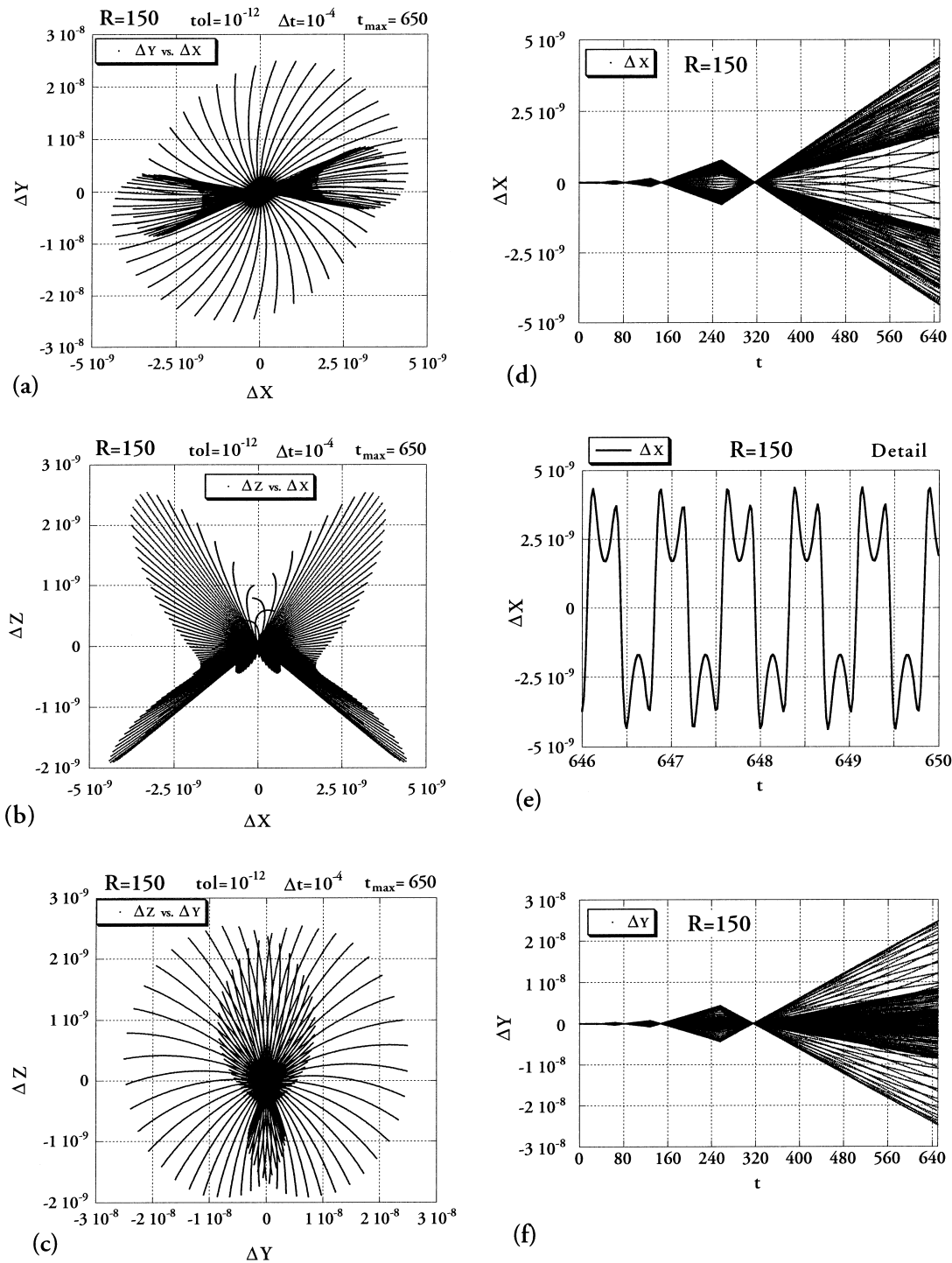


Fig. 8. Trajectory of differences between the computational (Adomian decomposition) and numerical (Runge–Kutta) solutions for a maximum computational time, $t_{max}=650$, corresponding to $\Delta t = 10^{-4}$ in the computational solution, $tol = 10^{-12}$ in the numerical solution, and $R = 150$. (a) Projection of trajectory's data points on the plane $\Delta Z = 0$, (b) projection of trajectory's data points on the plane $\Delta Y = 0$, (c) projection of trajectory's data points on the plane $\Delta X = 0$. (d) the solution of $\Delta X(t)$ projected on the time domain, (e) inset of the solution $\Delta X(t)$ projected on the time domain for $646 < t < 650$, (f) the solution of $\Delta Y(t)$ projected on the time domain. (Except for (e), the data points are not connected.)

and the envelope of the solution in the time domain also preserves a similar property. At this stage it is essential to get a realistic feeling of the dimensional values of time corresponding to $t_{\max} = 210$ and $t_{\max} = 650$ in order to understand the practical implications of continuing the evaluations for higher values of t_{\max} . We therefore convert the dimensionless time back to dimensional values by using a range of values of thermal diffusivity α_* corresponding to silicon oils ($\alpha_* \sim 10^{-7}$ m²/s), water ($\alpha_* \sim 1.5 \times 10^{-7}$ m²/s), air ($\alpha_* \sim 2.3 \times 10^{-5}$ m²/s) and some liquid metals ($\alpha_* \sim 6 \times 10^{-5}$ m²/s) and a range of length scales spanning from 0.01 (corresponding to some insulation layers), 0.1, 1 and upto 100 m (corresponding to convection in underground aquifers). The converted dimensional values of $t_{*, \max}$ corresponding to the dimensionless value of $t_{\max} = 210$ varies from ~ 18 and ~ 46 s for liquid metals and air, respectively, to ~ 2 and ~ 3 h for water and silicon oils, respectively, all filling a domain having a height of 0.01 m. When the domain's height increases to 1 m the corresponding dimensional value of $t_{*, \max}$ increases by a factor of 10^4 and becomes ~ 2 days, ~ 5.3 days, ~ 2.3 years and ~ 3.4 years for liquid metals, air, water and silicon oils, respectively. A further increase in the domain's height to 10 m causes a corresponding increase in $t_{*, \max}$ by a factor of 10^2 and brings all its values to be of an order of magnitude of between ~ 1 and 340 years. All these results increase by a factor of ~ 3.1 when the dimensionless value of t_{\max} becomes $t_{\max} = 650$. Clearly, there is no much point in looking at the behaviour of the results beyond these maximum time values as in practice they will be noticed on a "secular" time scale only, and no practical measurements can be taken over such a long time scale. Any experimental observations will detect a "perpetual transient" phenomenon and post-transient results, even if they exist, (or their divergence over the "secular" time scale), are of a much less relevance in this context.

6. Conclusions

A demonstration of the convergence conditions for Adomian decomposition method of solution to the Lorenz equations was presented for a wide range of values of the scaled Rayleigh number. A further evaluation of the accuracy of the decomposition method was undertaken by comparing its results with a numerical Runge–Kutta–Verner solution. The solutions clearly indicate that Adomian's decomposition method yields generally more accurate results than the numerical method, however both solutions agree up to 12–13 significant digits at subcritical conditions, and up to 8–9 significant digits at certain supercritical conditions.

The difference between the two solutions was presented as projections of trajectories in the state space, producing similar shapes that preserve under scale reduction or magnification, and are presumed to be of a fractal form.

Acknowledgements

One of the authors (P.V.) wishes to thank the Department of Mechanical Engineering at University of Natal-Durban, for the support during his Sabbatical leave which made this work possible, and the Foundation for Research Development (South Africa) for partially funding this study through the Competitive Industry Research Grant (CIPM-GUN2034039).

References

- [1] G. Adomian, A review of the decomposition method in applied mathematics, *J. Math. Anal. Appl* 135 (1988) 501–544.
- [2] G. Adomian, *Solving Frontier Problems in Physics: The Decomposition Method*, Kluwer Academic Publishers, Dordrecht, 1994.
- [3] P. Vadasz, Subcritical transitions to chaos and hysteresis in a fluid layer heated from below, *International Journal of Heat and Mass Transfer* 43 (2000) 705–724.
- [4] P. Vadasz, S. Olek, Weak turbulence and chaos for low Prandtl number gravity driven convection in porous media, *Transport in Porous Media* 37 (1) (1999) 69–91.
- [5] P. Vadasz, S. Olek, Route to chaos for moderate prandtl number convection in a porous layer heated from below, *Transport in Porous Media* (1999) (in press).
- [6] E.N. Lorenz, Deterministic non-periodic flows, *J. Atmos. Sci* 20 (1963) 130–141.
- [7] C. Sparrow, *The Lorenz Equations: Bifurcations, Chaos, and Strange Attractors*, Springer-Verlag, New York, 1982.
- [8] A.J. Lichtenberg, M.A. Lieberman, Regular and chaotic dynamics, in: *Applied Mathematical Sciences*, 2nd ed., vol. 38, Springer-Verlag, New York, 1992.
- [9] W.V.R. Malkus, Non-periodic convection at high and low Prandtl number, *Mem. Soc. R. Sci. Liege IV* (6) (1972) 125–128.
- [10] P. Vadasz, S. Olek, Transitions and chaos for free convection in a rotating porous layer, *Int. J. Heat Mass Transfer* 14 (11) (1998) 1417–1435.
- [11] S. Olek, An accurate solution to the multispecies Lotka–Volterra equations, *SIAM Review* 36 (1994) 480–488.
- [12] P. Vadasz, Local and global transitions to chaos and hysteresis in a porous layer heated from below, *Transport in Porous Media* 37(2) (1999) 213–245.
- [13] P. Yuen, H.H. Bau, Rendering a subcritical Hopf bifurcation supercritical, *J. Fluid Mechanics* 317 (1996) 91–109.

- [14] Y. Wang, J. Singer, H.H. Bau, Controlling chaos in a thermal convection loop, *J. Fluid Mechanics* 237 (1992) 479–498.
- [15] A. Repaci, Non-linear dynamical systems: on the accuracy of Adomian's decomposition method, *Appl. Math. Lett* 3 (1990) 35–39.
- [16] S. Wolfram, *Mathematica[®]: A System for Doing Mathematics by Computer*, 2nd ed., Addison-Wesley, Redwood City, CA, 1991 (Wolfram Research).
- [17] IMSL Library, *Fortran Subroutines for Mathematical Applications*, version 2, Houston, 1991.